http://dx.doi.org/10.5012/bkcs.2014.35.5.1523

Characterization of Band Gaps of Silicon Quantum Dots Synthesized by Etching Silicon Nanopowder with Aqueous Hydrofluoric Acid and Nitric Acid

Thu-Huong Le and Hyun-Dam Jeong*

*Department of Chemistry, Chonnam National Univesity, Gwangju 500-757, Korea. *E-mail: hdieong@chonnam.ac.kr*
Received December 3, 2013, Accepted January 31, 2014

Silicon quantum dots (Si QDs) were synthesized by etching silicon nanopowder with aqueous hydrofluoric acid (HF) and nitric acid (HNO_3). Then, the hydride-terminated Si QDs (H-Si QDs) were functionalized by 1-octadecene (ODE). By only controlling the etching time, the maximum luminescence peak of octadecyl-terminated Si QDs (ODE-Si QDs) was tuned from 404 nm to 507 nm. The average optical gap was increased from 2.60 eV (ODE-Si QDs-5 min) for 5 min of etching to 3.20 eV (ODE-Si QDs-15 min) for 15 min of etching, and to 3.40 eV (ODE-Si QDs-30 min) for 30 min of etching. The electron affinities (EA), ionization potentials (IP), and quasi-particle gap (ε_{gap}^{qp}) of the Si QDs were determined by cyclic voltammetry (CV). The quasi-particle gaps obtained from the CV were in good agreement with the average optical gap values from UV-vis absorption. In the case of the ODE-Si QDs-30 min sample, the difference between the quasi-particle gap and the average optical gap gives the electron-hole Coulombic interaction energy. The additional electronic levels of the ODE-Si QDs-30 min and ODE-Si QDs-15 min samples determined by the CV results are interpreted to have originated from the Si=O bond terminating Si QD.

Key Words : Silicon quantum dot, Electronic structure, Cyclic voltammetry, Quasi-particle gap, Optical gap

Introduction

Colloidal semiconductor nanocrystals or quantum dots of II, IV, and VI groups have received much attention for applications. As one of the most important semiconductor nanostructures, silicon quantum dots (Si QDs) are nontoxic and easily integrated into conventional process technologies. The electronic structure and size-dependent optical properties of the Si QDs play a key role in various applications, like solar cells,[1] optoelectronic devices,[2] and light-emitting devices.[3] Therefore, in order to utilize the Si QDs in sophisticated optoelectronic devices, exact knowledge of the size-dependent electronic structure parameters is required. The electronic structure parameters of Si QDs of various sizes can be estimated from scanning tunneling microscopy,[4] X-ray absorption spectroscopy,[5] and cyclic voltammetry (CV).[6] The CV method has been used in quantitative determination of electronic structure of CdSe QDs,[7] CdTe QDs,[8] and CdSeTe QDs[9] for several decades. The main advantage of the CV method is the operation with easier experimental conditions compared with other techniques such as X-ray absorption spectroscopy and scanning tunneling spectroscopy.

The process of charge transfer with quantum dots can be described in four way (Scheme 1):[6] (i) electron addition into a neutral QD (Scheme 1(a)), (ii) electron extraction from a neutral QD (Scheme 1(b)), (iii) simultaneous injection of an electron and a hole in two non-interaction QDs (Scheme 1(c)), (iv) creation of an interacting electron and hole pair in a single QD due to optical exciton (Scheme 1(d)). As shown in Scheme 1(a), by driving the potential of the working electrode to a more negative potential, the Fermi level of the working electrode reaches a level high enough to occupy vacant states on QDs in the electrolyte. In this case, an electron from the working electrode is transferred to the QDs, which is defined as the reduction processed. The energy require to load an electron from the working electrode is defined as the electron affinity (EA). Conversely (Scheme 1(b)), when the potential of the working electrode is scanned toward a more positive potential, an electron on QDs in the electrolyte will transfer to the working electrode, which is defined as the oxidation processed. The energy require to load an electron from QDs to working electrode is defined as ionization potential (IP).[7-10] The difference between the electron affinities (EA) and the ionization potentials (IP) is known as the quasi-particle gap (ε_{gap}^{qp}) which is energy

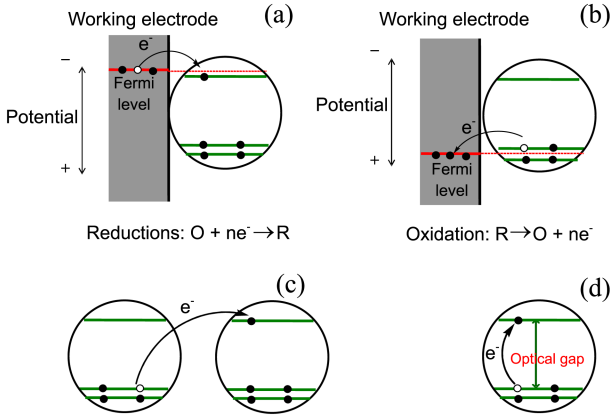

Scheme 1. Schematic representation of charge transfer processes: (a) electron addition into a neutral QD, (b) electron extraction from a neutral QD, (c) simultaneous injection of an electron and a hole in two non-interaction QDs, (d) creation of an interacting electron and hole pair in a single QD due to optical exciton.

required to produce a non-interaction electron-hole pair of QDs (Scheme 1(c)).[6] The quasi-particle gap (ε_{gap}^{qp}) is related the optical band gap (ε_{gap}^{opt}), corresponding to process in Scheme 1(d)) by equation (1):[10] $\varepsilon_{gap}^{opt} = \varepsilon_{gap}^{qp} - J_{e,h}$ (1). Where $J_{e,h}$ is the total coulomb interaction energy of electron-hole pair in a single QD. The optical band gap (ε_{gap}^{opt}) can be measured from spectroscopic data. The EA, IP, and the ε_{gap}^{qp} values of QDs can be determined from voltammetric experiments and estimated with reference to the vacuum level.

Recently, in order to study the size-dependent electronic structure parameters or quantum confinement effect of Si QDs, this laboratory has synthesized three sizes of Si QDs terminated by 1-octadecene. The physicists and chemists have reported about the synthesis of size-controlled and surface-functionalized Si QDs, such as chemical vapor deposition, plasma synthesis,[11] reverse micelle,[12] reduction $SiCl_4$ with various types of reducing agents,[13] and chemical etching.[14] For this study, we have applied the chemical etching method to silicon nanopowder to synthesize Si QDs, where the size of resultant silicon nanocrystals of the quantum dot regime was gradually decreased by increasing the etching time. The chemical etchant solution includes 48 wt % HF (1 mL), 60 wt % HNO_3 (1 mL), distilled water (2 mL), and methanol (2 mL).[15] The etching process was carried out with sonication. By controlling the etching time, the size of hydride-terminated silicon quantum dots (H-Si QDs) was tuned. Then, the H-Si QDs were functionalized by 1-octadecene (ODE) in toluene solvent at 110 °C for 12 h. The sizes of the octadecyl-capped Si QDs (ODE-Si QDs) were estimated by high-resolution transmission electron microscopy (HR-TEM). The electronic structure and optical properties of the various sizes of ODE-Si QDs have been investigated by cyclic voltammetry (CV), ultraviolet-visible (UV-vis) absorption spectroscopy, and photoluminescence spectroscopy (PL). UV absorption and photoluminescence spectra of three kinds of ODE-Si QD samples showed that the quantum confinement with decreasing QD size can be detected. By using cyclic voltammetric measurements, we have studied the electronic structure and confirmed the effect of size quantization of Si QDs. Although Si QDs were functionalized by 1-octadecene (ODE), oxidation phenomena on surface Si QDs were found, which was clearly confirmed by FT-IR (Figure 1). The additional electronic levels of the ODE-Si QDs-30 min and ODE-Si QDs-15 min samples determined by the CV results are interpreted to have originated from Si=O bond terminating Si QDs.

Experimental

Chemicals. Silicon nanopowder (Si NCs@SiO_2, KCC), 48% hydrofluoric acid (HF, Sigma-Aldrich), 60% nitric acid (HNO_3, Daejung), distilled water (H_2O), anhydrous methanol (Sigma-Aldrich), 99.8% anhydrous toluene (Sigma-Aldrich), 98% 1-ocadecene (ODE, Sigma-Aldrich), 99.5% dimethyl sulfoxide (DMSO, Daejung), tetrabutyl ammonium perchlorate (TBAP, Sigma-Aldrich), and silica-gel (SiO_2, 40-60 μm, Merck) were used in the experiments.

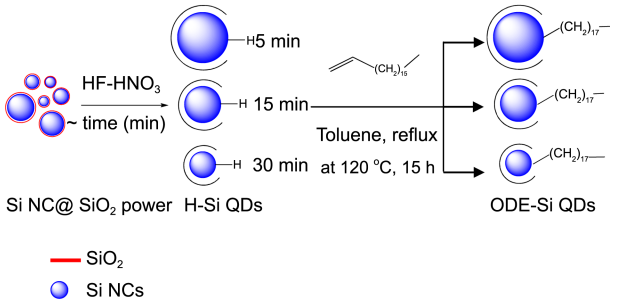

Scheme 2. Size-controlled synthesis of Si QDs by wet etching Si NCs@SiO_2.

Synthesis of Silicon Quantum Dots. The synthesis was prepared in a glove box filled with Ar gas, as summarized in Scheme 2. The hydride-terminated silicon quantum dots (H-Si QDs) were synthesized from Si NCs@SiO_2 by using the controlled chemical etching method reported by K. Sato.[15] The etching time was varied from 5 min to 15 min and 30 min. After completing the etching process, hydride-terminated Si QDs were isolated by extraction with 20 mL of anhydrous toluene. Then, 10 mL of 1-octadecene was added to the solution reaction. The reaction mixture was degassed by three cycles of evacuation and purging with argon, and then placed in a silicon oil bath heated at 120 °C for 15 h. After the thermal functionalization, the reaction mixture was filtrated to yield a clear, bright yellow. Next, all solvents was removed at 40 °C under reduced pressure by using rotary evaporator. The remaining capping molecules were separated by the column chromatography of silica-gel (40-63 μm) using hexane solvent. The product was obtained as yellow resin.

Characterization. UV-vis absorption spectra were obtained on an S-3150 UV-vis spectrometer (SCINCO, Korea). Photoluminescence spectroscopy was performed on a Flourolog-3 spectrometer with a 2-nm slit width for excitation monochromators. Fourier-transform infrared FT-IR spectroscopy was performed on a Spectrum 400 (PekinElmer, USA) to obtain the IR spectra of Si QDs. A 300 MHz FT-NMR spectrometer (Varian Inc, Palo Alto, CA) was used to obtain 1H-NMR spectra of the ODE-Si QDs. High-resolution transmission electron microscopy (HR-TEM) was done with a JEOL JEM-2100F operated at 200 kV.

Electrochemical Characterization: The cyclic voltammetric measurements were carried out at room temperature. After fixing the electrodes to the cell, Si QDs (3.5 mg) were first added to a cell containing DMSO (8 mL) and toluene (2 mL) premixed with tetrabutyl ammonium perchlorate (TBAP, net concentration 100 mM). The role of toluene was to enhance the dispersion ability of the QDs. Cyclic voltammetry was recorded with the help of IviumSoft version 2.1XX in a three-electrode system. Glassy carbon (GC, 3 mm diameter), Ag wire, and Pt wire were used as the working electrode, reference electrode, and counter electrode, respectively. All the potentials were calibrated to the reference potential of the vacuum level.

Results and Discussion

The surface chemistry of H-Si QDs was confirmed based on FT-IR spectroscopy. Figure 1 shows the presence of a Si-H stretching vibration mode of the H-Si QD sample at 2122.8 cm^{-1}. The peak at 2917.1 cm^{-1} was attributed to the C^{sp3}-H stretching vibration of the toluene solvent used in the extraction process of the H-Si QDs. The Si-O stretching vibration in the range of 1100 to 1000 cm^{-1} was also observed in the spectrum, which was due to the brief air exposure of the sample during preparation for FT-IR measurement.

The bonding of 1-octadecene onto the surface of ODE-Si QDs-5 min, ODE-Si QDs-15 min, and ODE-Si QDs-30 min were confirmed by the FT-IR graphs in Figure 1. For all three samples of Si QDs, the alkyl group on surface Si QDs including the asymmetric stretching, symmetric stretching, and in-plane bending or scissoring of the -CH_2- groups were obtained at 2917.1 cm^{-1}, 2846.9 cm^{-1}, and 1460.7 cm^{-1}. We observed a peak at 1277.0 cm^{-1} attributed to the symmetric bending vibration of Si-C.[16] The peaks at 1237.7 and 1160.0 cm^{-1} are attributed to the Si=O stretching vibration, which was in excellent agreement with the calculation By Y. J. Chabal.[17] The peaks between 1000-1100 cm^{-1} corresponded to Si-OR stretching vibrations and indicated that the oxidation of Si QD had occurred. The peaks at 1600-1700 cm^{-1} were attributed to the stretching of the C=C bond of the remaining capping.

The structure of ODE-Si QDs was further confirmed by NMR spectroscopy, as shown in Figure S2. In the ^{1}H-NMR spectra, two resonance protons (Si-CH_2-) and (-CH_3), are peaking distinguishably at 1.28 ppm and 0.90 ppm. The relative proton integral ratio of (Si-CH_2-) and (-CH_3) (1.14: 0.11) shows that the majority of the product is the octadecyl-terminated Si QDs.

As shown in the TEM images (Figure 2), we found a characteristic lattice spacing of 1.9 Å corresponding to a d-spacing of (220), confirming a diamond crystal structure.[18] From the size distribution depicted in Figure S2, we obtained the average diameters of the ODE-Si QD-5 min, DE-Si QD-15 min, and ODE-Si QD-30 min samples as 7.14 nm ± 3.5 nm, 3.0 nm ± 1.3 nm, and 2.05 ± 0.6 nm, respectively.

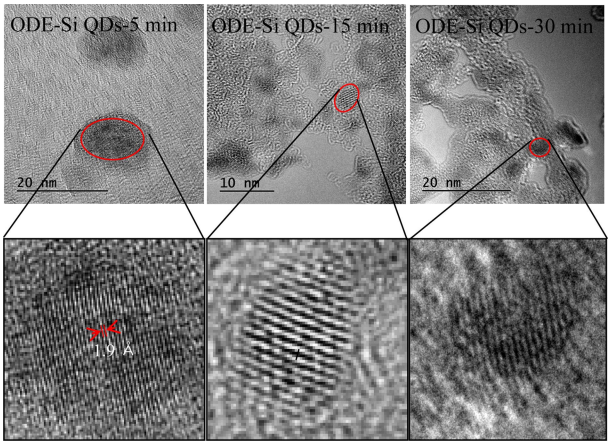

Figure 2. TEM images of ODE-Si QDs-30 min (2.05 nm), ODE-Si QDs-15 min (3.09 nm), and ODE-Si QDs-5 min (7.14 nm).

The optical properties of ODE-Si QDs synthesized with different etching times were investigated by UV-vis absorption spectroscopy, as shown in Figure 3(a). Clearly, when the

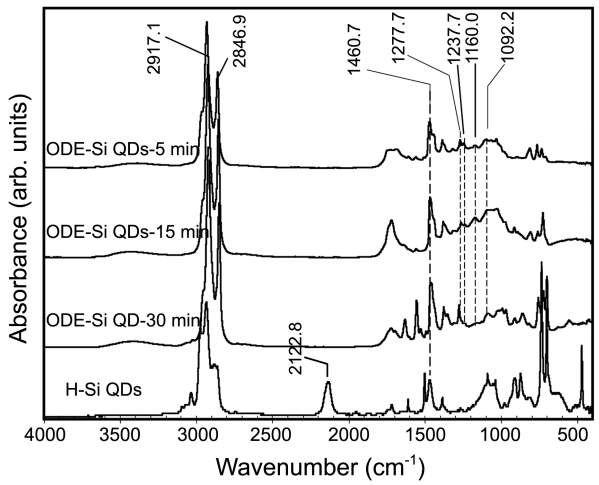

Figure 1. FT-IR spectra of H-Si QDs, ODE-Si QDs-30 min, ODE-Si QDs-15 min, and ODE-Si QDs-5 min.

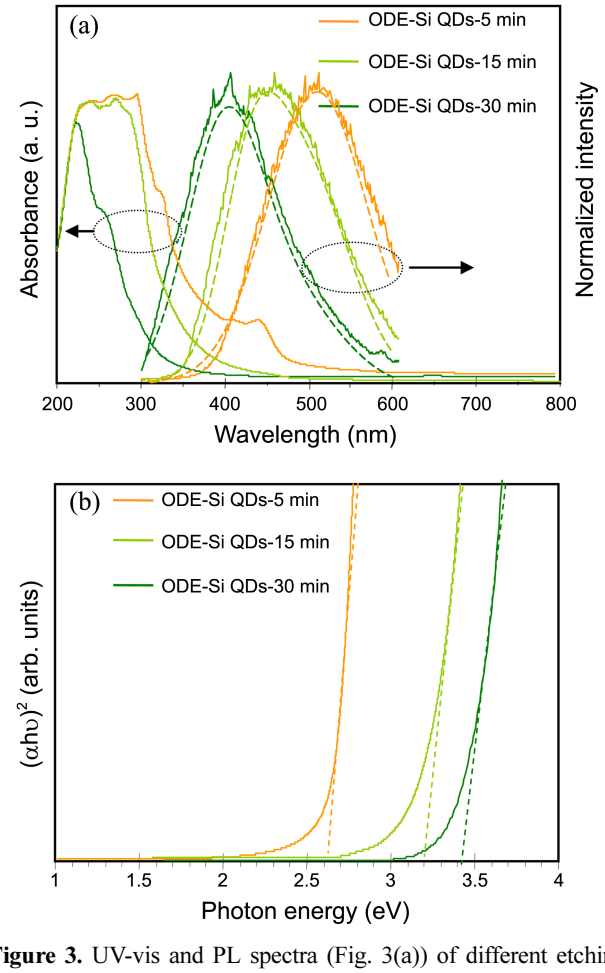

Figure 3. UV-vis and PL spectra (Fig. 3(a)) of different etching time of ODE-Si QDs. And Tauc plot (Fig. 3(b)) for the Si QDs for the case of 0.25 wt % concentration.

etching time varies from 5 min to 15 min and 30 min, the onset of the UV-vis absorption spectrum (Figure 3(a)) was blue-shifted from about 500 nm (ODE-Si QDs-5 min-0.25 wt % in hexane) and 450 nm (ODE-Si QDs-15 min-0.25 wt % in hexane) to about 400 nm (ODE-Si QDs-30 min-0.25 wt % in hexane). In Figure S3, the concentrations were given in weight. It is clear that the UV absorbance in the range above 400 nm was very low in the case of ODE-Si QDs-30 min, but it was enhanced in the cases of ODE-Si QDs-5 min and ODE-Si QDs-15 min.

The optical gaps of the ODE-Si QDs were estimated using Tauc plots of $(\alpha h\nu)^n$ *vs.* hυ as shown in Figure 3(b), in which α, h, and ν are the absorption coefficient, Planck constant, and frequency, respectively. The n value was taken as 2 since our Si QDs were assumed to have direct band gap characteristics.[18] The optical gaps of ODE-Si QDs-5 min, ODE-Si QDs-15 min, and ODE-Si QDs-30 min were estimated as 2.60 eV, 3.20 eV, and 3.40 eV, respectively, as shown in Figure 3(b). Distinctively, the optical gap was increased as the etching time increased, which was attributed to the quantum confinement effect.

Photoluminescence (PL) spectra of the three kinds of ODE-Si QDs under excitation with a wavelength of 290 nm were measured at room temperature in air (Figure 3(a)). By controlling only the etching time, the luminescence wavelength of the ODE-Si QDs can be tuned. The PL spectra (Figure 3(a)) shows a distinct difference in maximum peak energy at 507 nm (2.44 eV) for ODE-Si QDs-5 min, 455 nm (2.72 eV) for ODE-Si QDs-15 min, and 404 nm (3.07 eV) for ODE-Si QDs-30 min, which were lower values than the corresponding average optical band gap energies of the Si QDs with 2.6 eV (460 nm), 3.20 eV (360 nm), and 3.40 eV (329 nm), respectively. The difference between maximum peaks of PL (emission energy) and optical band gap (absorption energy) is attributed to Stokes shift phenomena. The radiation absorption of the QDs in the ground state configuration induces a transition between the HOMO and LUMO levels. A transition is followed by a relaxation in the excited state configuration, increasing distorted geometries and giving a new LUMO and HOMO, with an energy difference that was smaller than that in the ground state geometry. Therefore, the emission energy was lower than the absorption energy. PL spectra show the relationship between the maximum peak energies (in eV) and etching times (in min). The peak energy was increased as the etching time increased, which was attributed to the quantum confinement effect.

In the present chemical etching solution process, two main reaction steps were carried out. The first step was the surface oxidation of the Si nanopowder. The surface of silicon embedded in the nanopowder was oxidized by HNO_3 molecules ($3Si + 4HNO_3 \rightarrow 3SiO_2 + 4NO + 2H_2O$). The second step was the dissolution of the oxidized region by HF molecules ($SiO_2 + 6HF \rightarrow H_2SiF_6 + 2H_2O$). The SiO_2 regions consisting of the oxidized surfaces and original SiO_2 phases were completely removed, and then the Si atoms reappeared on the etched surface. The overall reaction was written as the following equation: $3Si + 4HNO_3 + 18HF \rightarrow 3H_2SiF_6 + 4NO + 8H_2O$.[15] As a result, the size of Si QDs was gradually decreased with the increase in the etching time, and the wavelength of the maximum peak intensity in the PL spectra was decreased.

The cyclic voltammetry (CV) has been successfully performed to elucidate the electronic structure of QDs such as CdTe and CdSe QDs.[6-8] This was the reason why we have used cyclic voltammetry to study the electronic structure of Si QDs with different sizes. Cyclic voltammetry is dynamic electrochemical method, where current-potential curves were recorded at defined scant rate. In the current-potential curves, the reduction potential and oxidation potential were expected to give respective cathodic peaks (E_c) (corresponding to the electron affinity EA) and anodic peaks (E_a) (corresponding to the ionization potential IP).[7-19] The difference between cathodic peaks E_c and anodic peaks E_a was regarded as a quasi-particle gap (ε_{gap}^{qp}).[6] In order to estimate the electron affinities (EA) and the ionization potentials (IP) versus the vacuum level, we used Eqs. (2) and (3).[19]

$$EA = -(E_c + 4.14)\ \text{eV} \quad (2)$$

$$IP = -(E_a + 4.14)\ \text{eV} \quad (3)$$

E_a and E_c are the anodic and cathodic peaks relative to the Ag/0.01 M $AgNO_3$ reference electrode. The value of 4.14 was the difference between the vacuum level potential of the normal hydrogen electrode (NHE = 4.44 eV) and the potential of the Ag/0.01 M $AgNO_3$ reference electrode.[19]

Figure 4 shows the CV graphs recorded on ODE-Si QDs for 5 min, 15 min, and 30 min of sample etching time in TBAP-toluene-dimethyl sulfoxide electrolyte solution and reference solution without Si QDs with a scan rate of 300 mVs^{-1}. The 5 min and 15 min samples had currents around 10 μA. Meanwhile, currents around 10 μA and 1 μA were applied to the instrument for the 30 min sample. In the Figure S4, compared with reference scan without Si QDs at small scan region, several anodic and cathodic peaks can see more clearly in the voltammograms of the QDs. However, the intensities of the anodic and cathodic peaks for the 5 min, 15 min, and 30 min samples were quite broad and increased intensity of the peak, respectively (Figure 4). We hold that this was related to the size distribution of Si QDs.[10-20] As illustrated in Figure S2, the size distribution of ODE-Si QDs-15, ODE-Si QDs-30 min and especially the ODE-Si QDs-5 min samples were large, which affected CV measurements. Therefore, the intensity of the anodic and cathodic peaks was low and broad.

The values of EA, IP, ε_{gap}^{qp} from CV (Figure S4) along with the optical band gap (Figure 2(b)) and maximum peaks PL (Figure 2(a)) are summarized in Table 1. The quasi-particle gap (ε_{gap}^{qp}) of ODE-Si QDs estimated from cathodic and anodic peaks was in accordance with the average optical gap values determined from the UV-vis absorption spectra by the Tauc-plot (Figure 2(b)). Table 1 show that the quasi-particle gap increases with decreases in the particle size. This was attributed to the quantum confinement of the

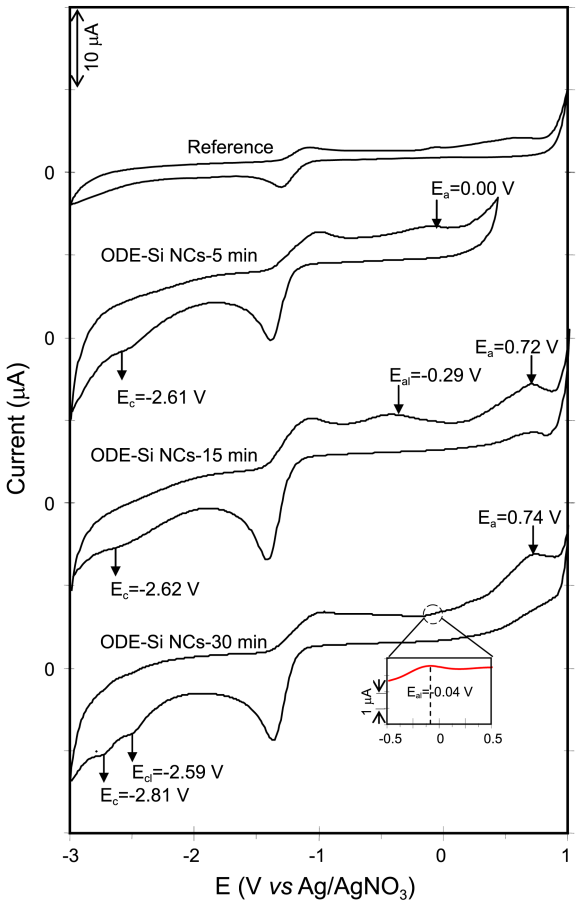

Figure 4. Cyclic voltammograms recorded on working electrode of different etching times for ODE-Si QDs and electrolyte solution without Si QDs. TBAP (100 mM) is used as supporting electrolyte and the scan rate is 300 mVs^{-1}. E_a and E_c denote the anodic and cathodic peaks, respectively. The potentials are calibrated versus the $Ag/AgNO_3$ electrode.

Table 1. Detail of electronic structure parameters, namely the electron affinities (EA), the ionization potentials (IP), the average optical gaps, maximum peak energy and quasi-particle gap of different etching time of ODE-SiQDs. The e_1 and h_1 positions are calibrated to the vacuum level

sample	Average optical gap [eV]	Max peak PL [eV]	EA *vs* vacuum	IP *vs* vacuum	ε_{gap}^{qp} [V]
5 min	2.60	2.44	−1.53	−4.14	2.61
15 min	3.20	2.72	−1.52	−4.86	3.34
30 min	3.40	3.07	−1.33	−4.88	3.55

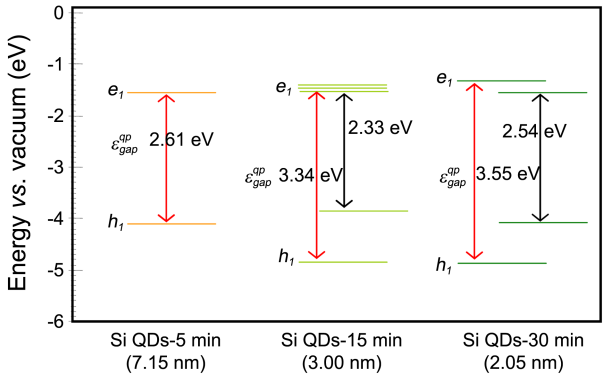

Figure 5. The electronic structure parameters of three kinds of Si QDs were obtained from CV.

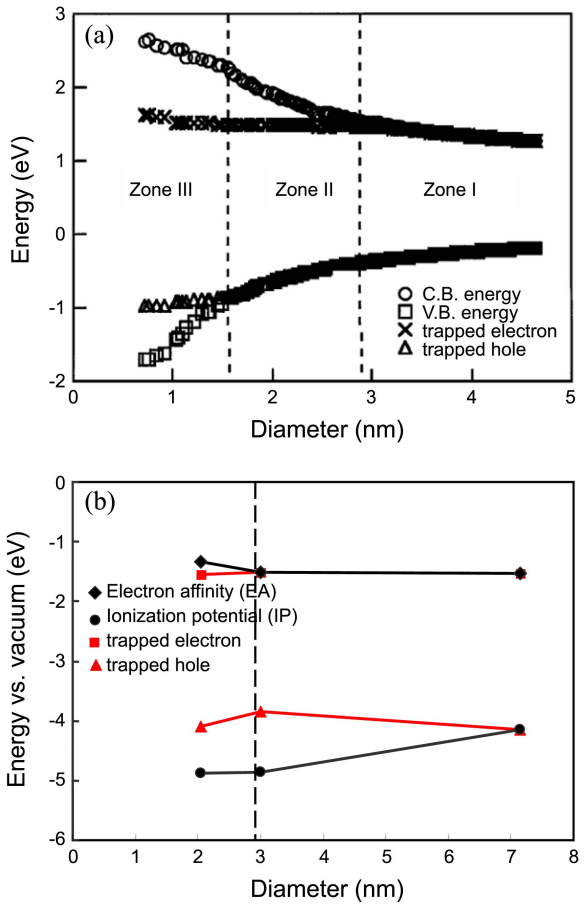

Figure 6. The values of electron affinity and ionization potential of three kinds of Si QDs as a function of size, obtained froms CV, shown in Figure 6(b). For comparision, the Wolkin results[21], shown in Figure 6(a).

charge. In addition, in the 5 min sample, the quasi-particle gap and optical gap values matched each other very well. However, the difference between the quasi-particle gap and optical gap value were 0.14 eV for the 15 min sample, and 0.15 eV for the 30 min sample, which was attributed to the significant electron-hole Coulombic interaction energy for the small QDs.[6]

In Figures 4-5, for the 5 min sample, the new states were not observed. Even the FT-IR results of the ODE-Si QDs-5 min sample show an oxidative surface state on Si QDs (Si=O).[17] Because the size of the ODE-Si QDs-5 min sample was big at 7.14 (nm), the optical band gap of the 5 min sample was narrower than the gap from the oxidation state (Si=O) on the surface of Si QDs. Thus, we just obtained the electron affinity, ionization potential, and quasi-particle gap values. However, the new electronic states were observed at E_{a1} = −0.29 (V) for ODE-Si QDs-15 min and at E_{a1} = −0.04

(V) and E_{a1} = −2.59 (V) for ODE-Si QDs-30 min. The calculated gap of the electronic states were 2.33 (eV) and 2.54 (eV), respectively, for ODE-Si QDs-15 min and ODE-Si QDs-30 min. We propose that these electronic states are consistent with the oxidative surface state on Si QDs (Si=O). The "oxidation state" was confirmed by the FT-IR results. As mentioned above, the FT-IR results (Figure 1) of the ODE-Si QDs-15 min and ODE-Si QDs-30 min showed the presence of Si=O stretching at 1237.7 and 1160.0 cm^{-1}, respectively.[17] As shown in Figures 6(a-b), the electronic structure of Si QDs with the oxidation state (Si=O) on their surface has been actively debated.[21] Wolkin reported on the electronic state in Si nanocrystals as a function of size and surface passivation (Figure 6(a)). Depending on the size of the cluster, three different recombination mechanisms were suggested. In zone III, the size of cluster was smaller than 2 nm, and the recombination of the Si cluster occurred *via* trapped excitons. In zone II, the size of the cluster was bigger than 2 nm and smaller than 3 nm and the recombination involves trapped electrons and free holes. In zone I, the size of the cluster was bigger than 3 nm, and recombination was *via* free excitons.[21] In our current study (Figure 6(b)), for the ODE-Si QDs-15 min sample, its size was 3 nm in zone II of Wolkin's report. So, this sample is thought to have electronic energy levels providing trap hole states. For the case of ODE-Si QDs-30 min (size 2.05 nm), the optical band gap was larger. Therefore, in the CV (Figure 6(b)) of the ODE-Si QDs-30 min sample, we can see redox peaks due to the intergap electronic energy levels of the oxidation state (Si=O), which was assigned to trapped electron and trapped hole states, in addition to the band-related energy levels in Si QDs.

Based on UV-vis absorption spectroscopy and PL, we have concluded that the CV is a more powerful technique to identify electronic structure and trap states on Si QDs. The CV method can be applied to the syntheses and characterizations of various kinds of Si QDs.

Conclusion

Different sizes of Si QDs were synthesized by etching silicon nanopowder with aqueous hydrofluoric acid (HF) and nitric acid (HNO_3). UV-vis absorption spectroscopy and PL results showed that the sizes of the Si QDs were decreased with the increased etching time. By using cyclic voltammetric measurements, the electronic structure of the Si QDs was studied in a quantitative manner, where the quasi-particle gap (ε_{gap}^{qp}) is similar to the average optical gap values from the UV-vis absorption spectroscopy. The energy level positions due to the oxidative surface state (Si=O) were determined from the CV measurement.

Acknowledgments. This research was supported by the Basic Science Research Program through the National Research Foundation of Korea (NRF) funded by the Ministry of Education, Science and Technology (No. 2012R1A1A2039579). This was financially supported by Chonnam National University, 2012.

References

1. Kamat, P. V. *J. Phys. Chem. C* **2008**, *112*, 18737-18753.
2. Salafsky, J. S. *Solid-State Electronics* **2001**, *45*, 53-58.
3. Peralvarez, M.; Carreras, J.; Barreto, J.; Morales, A.; Dominguez, C.; Garrido, B. *Appl. Phys. Lett*. **2008**, *92*, 241104.
4. Zaknoon, B.; Gap, B. *Nano Lett*. **2008**, *8*, 1689-1694.
5. Buuren, T. V.; Dinh, L. N.; Chase, L. L.; Siekhaus, J. W.; Terminello, L. J. *Phys. Rev. Lett.* **1998**, *80*, 3803-3806.
6. Inamdar, S. N.; Ingole, P. P.; Haram, S. K. *ChemPhysChem.* **2008**, *9*, 2574-2579.
7. Erol, K.; Bucking, W.; Sven, A.; Giernoth, R.; Nann, T. *ChemPhysChem.* **2006**, *7*, 77-81.
8. Haram, S. K.; Kchirsagar A.; Gujarathi, Y. D.; Ingole, P. P.; Nene, O. A.; Markad, G. B.; Nanavati, S. P. *J. Phys. Chem. C* **2011**, *115*, 6243-6249.
9. Hou, B.; Parker, D.; Kissling, G. P.; Jones, J. A.; Chern, D.; Fermin, D. J. *J. Phys. Chem. C* **2013**.
10. Amelia, M.; Lincheneau, C.; Silvi, S.; Credi, A. *Chem. Soc. Rev.* **2012**, *41*, 5728-5743.
11. Gupta, A.; Swihart, M. T.; Wiggers, H. *Adv. Funct. Master*. **2009**, *19*, 696-703.
12. Tilley, R. D.; Warner, J. H.; Yamamoto, K.; Matsui, I.; Fujimori, H. *Chem. Commun.* **2005**, *14*, 1833.
13. Sudeep, P. K.; Page, Z.; Emrick, T. *Chem. Commun*. **2008**, 6126-6127.
14. Nunez, J. R. R.; Kelly, J. A.; Henderson, E. J.; Veinot, J. G. C. *Chem. Matter*. **2012**, *24*, 346-352.
15. Sato, R.; Tsuji, H.; Hirakuri, K.; Fukata, N.; Yamauchi, Y. *Chem. Commun*. **2009**, 3759-3761.
16. Yang, C. S.; Bley, R. A.; Kauzlarich, S. M.; Lee, H. W. H.; Delgado, G. R. *J. Am. Chem. Soc*. **1999**, *121*, 5191-5195.
17. Chabal, J. Y.; Raghavachari, K.; Zhang, X.; Garfunkel, E. *Phys. Rev. B* **2002**, *66*, 161315.
18. Mai, X. D.; Dao, D. T.; Sohee, J.; Hyun, D. J. *Chem. Asian J.* **2013**, *8*, 653-664.
19. Kucur, E.; Riegler, J.; Urban, G. A.; Nann, T. *J. Chem. Phys. Vol.* 22 July **2003**, *119*(4).
20. Dissanayake, D. M. N. M.; Lutz, T.; Curry, R. J.; Silva, S. R. P. *Appl. Phys. Lett*. **2008**, *93*, 043501.
21. Wolkin, V. M.; Jorne, J.; Fauchet, M. P. *Phys. Rev. Letter*. **1999**, 82.